Automatic Detection Method of Localized Pavement Roughness Using Quarter Car Model by Lifting Wavelet Filters

Kazuya Tomiyama[1+], Akira Kawamura[1], and Tateki Ishida[2,]

Abstract: Causative pavement cracks in surface roughness require the functional evaluation derived from road profile data. This study examines an automatic detection method of transverse cracks on a surface profile in terms of a quarter car (QC) filtered roughness profile by lifting wavelet filters. Lifting wavelet filters are adaptive biorthogonal wavelet filters containing free parameters. In this study, we design a set of lifting wavelet filters for detecting severe cracks from the roughness profile. The set of filters includes free parameters that are intended to emphasize causative crack characteristics in the roughness profile. According to the results of adapting the filters to the roughness profile, the locations of severe cracks are identified, whereas locations that are not related to the QC response are not detected. Therefore, we conclude that the performance of the lifting wavelet filters contributes to automatic distress detection using response type profiling systems.

Introduction

Surface roughness of a pavement is an important factor for determining maintenance and rehabilitation needs of road networks. Rough pavements seriously reduce the performance of a road in respect of the response from road users regarding ride quality. Localized surface distress such as cracks may lead to increase pavement roughness by shaping steps around them. Road administrators are required to identify locations that need the maintenance and rehabilitation of localized roughness condition based on the quantitative monitoring of the surfaces. Many road administrators have developed profiling systems based on the vehicle vibration response called RTRRMS (Response Type Road Roughness Measuring System) since the International Roughness Index (IRI) has become the standard scale of predicting roughness condition in many countries in the world. This type of profiling system is usually intended to measure the IRI based on a quarter car (QC) model [1]. Although modern technologies of profiling with better sensors have contributed to measure surface profiles and to calculate the IRI, the application method for detecting localized surface distress are not well established.

Conventional detection algorithms for detecting localized surface distress such as convolution- and Fourier- based filters can pass the sinusoids keeping positive (e.g. bumps) and negative (e.g. cracks) amplitude for target wavelengths, that is, these algorithms are non-directional. A potential way to overcome this inadequacy concerning the detection algorithm is the wavelet transform. The algorithm of the wavelet transform is correlating and comparing the signal with various shifted and stretched versions of small waves localized in both time/distance and frequency called wavelets that

are constituted from a basic function [2]. By choosing a suitable basic function for an analyzed wave, this algorithm allows us to detect only wanted profile features and eliminate unwanted information of the profile by using a directional algorithm. A major remaining problem in the wavelet transform has been wise selection of a basic function suitable for profile analyses. The basic function affects the result of the transformation. Its design is, however, difficult for the sake of satisfying various restrictions such as an orthogonal condition [3]. Although the wavelet transforms have found many applications in evaluating road surface properties [4, 5], an optimum basic function for the purposes has been unknown. Since second generation wavelets based on the lifting scheme were proposed [6], this problem has been solved. A concept of the lifting scheme concentrates on the ability of lifting to enhance an existing wavelet transform by adding desirable properties to original basic functions [7]. This enables us to construct lifting wavelet filters that are adaptive biorthogonal wavelet filters containing controllable free parameters [8].

This study examines an automatic detection method of localized surface roughness by developing lifting wavelet filters appropriate for pavement monitoring using QC-based response type systems. In this study, we design a set of lifting wavelet filters for detecting causative transverse cracks in quarter car filtered roughness profile as an practical example. Cracks do not necessarily affect a vehicle because they are usually very narrow compared to the length of a tire contact patch. However, severe cracks may lead to increase roughness by shaping steps around them. In any pavement monitoring activity, the latter type of crack must be detected. For the purpose of this study, profiles of asphalt concrete pavements obtained from the Specific Pavement Studies 5 (SPS-5) project in the Long Term Pavement Performance (LTPP) program are used.

Monitoring Theory Using QC Algorithm

Over View of the QC Model

[1] 165 Koen-cho, Kitami, 090-8507 Japan.

[2] 1-3 Hiragishi, Toyohira-ku, Sapporo, 062-8602 Japan.

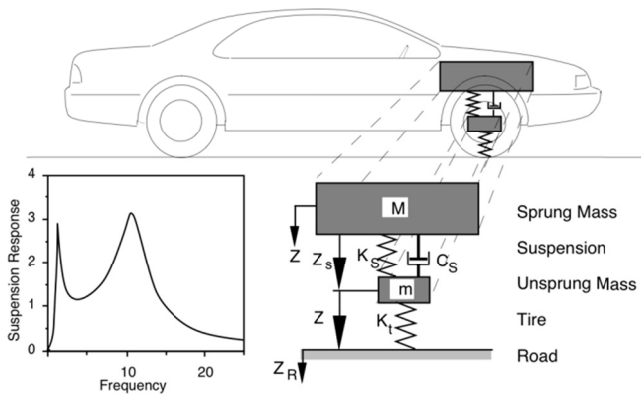[+] Corresponding Author: E-mail tomiyama@mail.kitami-it.ac.jp
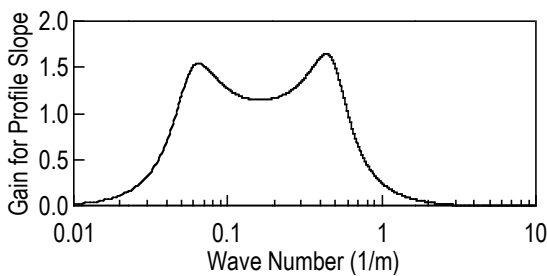
Fig. 1. Quarter-Car Model [9]

Fig. 2. QC Filter.

The QC model is a mathematical model of a vehicle that represents a body and a single wheel (Fig. 1) [9]. The IRI can be calculated by use of the QC model applied to a measured longitudinal road profile. The QC model predicts the spatial derivative of suspension stroke in response to a profile using standard settings called Golden Car Parameters for speed and the vehicle properties for Fig. 1. Since QC-based surface measurement systems have been developed, an automatic distress detection theory can contribute to efficient pavement monitoring activities.

QC Filter

The mathematical procedure in calculating IRI includes two filters: a moving average filter that reduces tire envelope characteristics and a QC filter shown in Fig. 2 that weights the wavelengths of a slope profile between 0.1 and 100m to gain the roughness characteristics. The QC filter removes the influence of individual suspension response for any profiling systems. As the result, the filtered profile indicates a QC filtered slope profile (a roughness profile) that has units of slope (mm/m, in/mi, etc.). This study examines a method for detecting severe cracks in a roughness profile that needs to be evaluated from functional viewpoint.

Distress Detection Method by Lifting Wavelet Filters

In the wavelet transformations, a profile is analyzed at different frequency bands with different resolution by decomposing the signal into components consisting of a coarse approximation (low frequency component) supplemented by detailed information (high frequency component). The approximation can be then further

decomposed to provide more detailed information. This means that wavelet transforms, especially for discrete transform, can perform multiresolution analysis using a fast pyramid algorithm. Lifting wavelet filters are biorthogonal wavelet filters containing controllable free parameters constructed from initial biorthogonal wavelet filters based on the lifting scheme theory. Free parameters can be learnt from training signals that include desired profile features such as pavement cracks. The following are the details of a detection theory based on the lifting scheme theory.

Wavelet Decomposition of a Profile.

Let c_l^1 denote a profile with distance parameter l. Using multiresolution analysis in a wavelet theory, the profile can be decomposed into low frequency and high frequency components as follows:

$$\hat{c}_m^0 = \sum_l \tilde{\lambda}_{l-2m} c_l^1, \tag{1}$$

$$\hat{d}_m^0 = \sum_l \tilde{\mu}_{l-2m} c_l^1, \tag{2}$$

where $\tilde{\lambda}_m$ and $\tilde{\mu}_m$ are called decomposition filters. Conversely, the original profile can be reconstructed from the low frequency and high frequency components $\hat{c}_m^0$ and $\hat{d}_m^0$ by the formula

$$c_l^1 = \sum_m \lambda_{l-2m} \hat{c}_m^0 + \sum_m \mu_{l-2m} \hat{d}_m^0, \tag{3}$$

where λ_m and μ_m are called reconstruction filters. For later convenience, the decomposition and reconstruction filters are denoted as

$$h_{k,l}^{old} = \lambda_{k-2l}, \quad g_{m,l}^{old} = \mu_{l-2m}, \tilde{h}_{k,l}^{old} = \tilde{\lambda}_{k-2l}, \quad \tilde{g}_{m,l}^{old} = \tilde{\mu}_{l-2m}. \tag{4}$$

The tuple of these filters $\{h_{k,l}^{old}, \tilde{h}_{k,l}^{old}, g_{m,l}^{old}, \tilde{g}_{m,l}^{old}\}$ satisfies the following conditions

$$\sum_l h_{k,l}^{old} \tilde{h}_{k',l}^{old} = \delta_{kk'}, \quad \sum_l g_{m,l}^{old} \tilde{h}_{k,l}^{old} = 0,$$
$$\sum_l h_{k,l}^{old} \tilde{g}_{m,l}^{old} = 0, \quad \sum_l g_{m,l}^{old} \tilde{g}_{m',l}^{old} = \delta_{mm'}. \tag{5}$$

which are called biorthogonal conditions. Where δ indicates Kronecker delta.

Lifting Wavelet Filters

Let $\{h_{k,l}^{old}, \tilde{h}_{k,l}^{old}, g_{m,l}^{old}, \tilde{g}_{m,l}^{old}\}$ denote initial biorthogonal wavelet filters. A new set of biorthogonal wavelet filters $\{h_{k,l}, \tilde{h}_{k,l}, g_{m,l}, \tilde{g}_{m,l}\}$ is defined as follows:

$$h_{k,l} = h_{k,l}^{old} + \sum_m \tilde{s}_{k,m} g_{m,l}^{old}, \quad \tilde{h}_{k,l} = \tilde{h}_{k,l}^{old},$$
$$g_{m,l} = g_{m,l}^{old}, \quad \tilde{g}_{m,l} = \tilde{g}_{m,l}^{old} - \sum_k \tilde{s}_{k,m} \tilde{h}_{k,l}^{old}, \tag{6}$$

where $\tilde{s}_{k,m}$ denote free parameters, $\tilde{h}_{k,l}$ and $\tilde{g}_{m,l}$ indicate low- and

high- pass decomposition filters, and $h_{k,l}$ and $g_{m,l}$ indicate low- and high- pass reconstruction filters, respectively. This algorithm can create a new filter set suitable for desirable features in a sequence of analyzed profile data by adjusting free parameters. The learning method for adjusting the free parameters is described in the next section. The biorthogonal conditions of a new filter set are as follows:

$$\sum_l h_{k,l}\tilde{h}_{k',l} = \delta_{kk'}, \quad \sum_l g_{m,l}\tilde{h}_{k,l} = 0, \sum_l h_{k,l}\tilde{g}_{m,l} = 0, \quad \sum_l g_{m,l}\tilde{g}_{m',l} = \delta_{mm'} \quad (7)$$

Learning Method of Free Parameters

As shown in Eq. (6), high-pass filters, rather than low-pass filters are modified in the decomposition process. Where an input profile is again denoted as c_l^1, new high frequency components by applying the new high-pass decomposition filters can be written as

$$d_m^0 = \sum_l \tilde{g}_{m,l} c_l^1. \quad (8)$$

This can be substituted based on Eq. (6) as follows:

$$d_m^0 = \sum_l (\tilde{g}_{m,l}^{old} - \sum_k \tilde{s}_{k,m}\tilde{h}_{k,l}^{old})c_l^1 \quad = r_m - \sum_k a_k\tilde{s}_{k,m} \quad (9)$$

where r_m and a_k indicate the high and low frequency components resulted from the decomposition using the old filters, that is,

$$r_m = \sum_l \tilde{g}_{m,l}^{old} c_l^1, \quad a_k = \sum_l \tilde{h}_{k,l}^{old} c_l^1. \quad (10)$$

Free parameters $\tilde{s}_{k,m}$ can be determined so as to vanish the high frequency component d_m^0 in Eq. (9). In other words, desired features of the input profile can be detected by putting

$$d_m^0 = r_m - \sum_k a_k\tilde{s}_{k,m} = 0. \quad (11)$$

To learn the free parameters $\tilde{s}_{k,m}$, the algorithm requires $2n$ training signals $c_l^{1,v}$ ($v = 1,2,\dots,2n$) that include desired features such as pavement cracks. Then, the following condition is imposed:

$$\sum_{k=m-n}^{m+n} a_k^v \tilde{s}_{k,m} - r_m = 0, \quad v = 1,2,\dots,2n \quad (12)$$

where

$$r_m^v = \sum_l \tilde{g}_{m,l}^{old} c_l^{1,v}, \quad a_m^v = \sum_l \tilde{h}_{k,l}^{old} c_l^{1,v}. \quad (13)$$

Although the number of equations in Eq. (12) is 2n, unknown variables $\tilde{s}_{k,m}$ are 2n+1. However, the following equation is consequentially identified because the summation of a high-pass filter must be zero, that is,

$$\sum_l \tilde{g}_{m,l} = \sum_l (\tilde{g}_{m,l}^{old} - \sum_{k=m-n}^{m+n} \tilde{s}_{k,m}\tilde{h}_{k,l}^{old}) = 0. \quad (14)$$

Since $\tilde{g}_{m,l}^{old}$ satisfy $\sum_l \tilde{g}_{m,l}^{old} = 0$, this condition is equivalent to

$$\sum_{k=m-n}^{m+n} \tilde{s}_{k,m} = 0. \quad (15)$$

Summarizing Eqs. (12) and (15) in the matrix form results in the following equation:

$$\begin{bmatrix} a_{m-n}^1 & a_{m-n+1}^1 & \cdot & a_{m+n}^1 \\ a_{m-n}^2 & a_{m-n+1}^2 & \cdot & a_{m+n}^2 \\ \cdot & \cdot & \cdot & \cdot \\ \cdot & \cdot & \cdot & \cdot \\ a_{m-n}^{2n} & a_{m-n+1}^{2n} & \cdot & a_{m+n}^{2n} \\ 1 & 1 & \cdot & 1 \end{bmatrix} \begin{bmatrix} \tilde{s}_{m-n,m} \\ \tilde{s}_{m-n+1,m} \\ \cdot \\ \cdot \\ \tilde{s}_{m+n-1,m} \\ \tilde{s}_{m+n,m} \end{bmatrix} = \begin{bmatrix} r_m^1 \\ r_m^2 \\ \cdot \\ \cdot \\ r_m^{2n} \\ 0 \end{bmatrix}. \quad (16)$$

This equation can be solved by the Gaussian elimination. Substituting the solutions $\tilde{s}_{k,m}$ into Eq. (6), learnt adaptive wavelet filters can be produced.

Detection Theory

For detecting a profile feature that is similar to the training signals, first, the high-frequency components $\hat{d}_m^0$ and d_m^0 are calculated by the old and new high-pass wavelet filters $\tilde{g}_{m,l}^{old}$ and $\tilde{g}_{m,l}$ from c_l^1 by use of Eqs. (2) and (8). Here, remind that the free parameters $\tilde{s}_{k,m}$ of the new wavelet filters $\tilde{g}_{m,l}$ are optimized to vanish d_m^0 at the locations of the desired profile features. A possible strategy is to find the location m that makes $d_m^0 = 0$. Unfortunately, this strategy may detect the distance m other than the desired feature that their high frequency components are almost zero for both $\hat{d}_m^0$ and d_m^0. To avoid this kind of false detections, Takano et al. [8] suggested the method that search c_l^1 to find the location m so as to maximize the quantity

$$I_m = \left| \hat{d}_m^0 \right| - \left| d_m^0 \right| \quad (17)$$

When the value $I_m \geq 0$ is larger than a certain threshold value, the location m is regarded as the desired feature point. A schematic description of the detection theory is shown in Fig. 3. A threshold depends on the grade of a road and its control strategy.

An Application Case Study for Crack Detection

For an application case study, this chapter describes development of a set of lifting wavelet filters for detecting causative localized distress such as transverse cracks in quarter car filtered-roughness profile.

Analyzed Profile Data

A SPS-5 project in the LTPP program includes nine core test sections. The test sections have the same characteristics for all
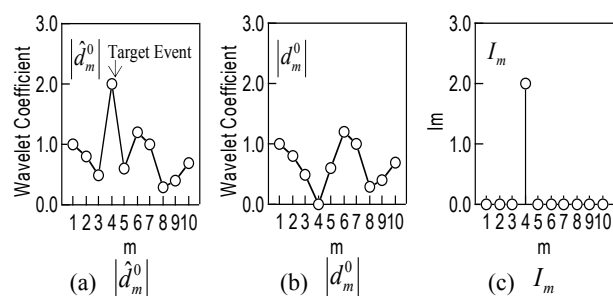
Fig. 3. A Schematic Description of the Detection Theory.

Fig. 5. QC Filtered Roughness Profile (Arrows Indicate the Location of Training Signals).

Code: 04) that have recorded severe transverse cracks. The profile data are available from LTPP Products Online [11]. Two profiles as shown in Fig. 4 which are identified as Profile 1 and 2 in this paper were extracted from the LTPP Products Online.

Profile 1 was measured in September 1990 that was immediately after overlay. Thus, no crack is found in the profile. Profile 2 was measured in December 1997. In 1997, the manual distress survey was performed as well as the profile measurement, and reported some transverse cracks.

Training Signals

Fig. 5 shows the roughness profile based on the QC filter of Profile 2. A glance at the figure indicates that the roughness profile emphasizes the effect of the severe cracks in the profile. However, detailed locations of the cracks can be hardly identified. To overcome this difficulty, the shapes of the roughness profile on severe six cracks ($2n = 6$) that are marked by arrows in Figs. 4 and 5 are learnt as training signals. The trained cracks appear as narrow
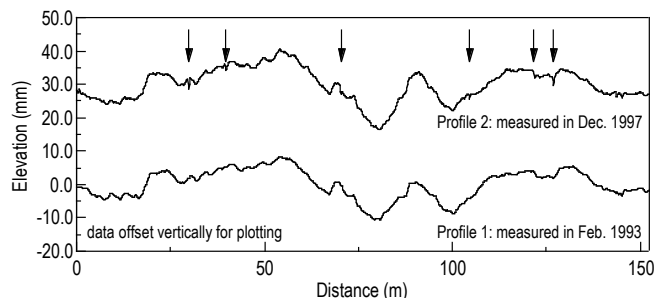

Fig. 4. Analyzed Profiles (Arrows Indicate the Location of Training Signals).

SPS-5 sites throughout the LTPP study as well as the same guideline for construction, maintenance and rehabilitation. Eight test sections (Section 502-509) are experimental sections, and one section (Section 501) is the control section that received only routine maintenance. Each section is about 152.4 m long, and the profiles are taken at 150 or 152 mm intervals that have been resampled at an interval of 150 mm in the present study. More detailed information of the SPS-5 project is given elsewhere [10]. The present study uses the data from Section 509 in Arizona (State
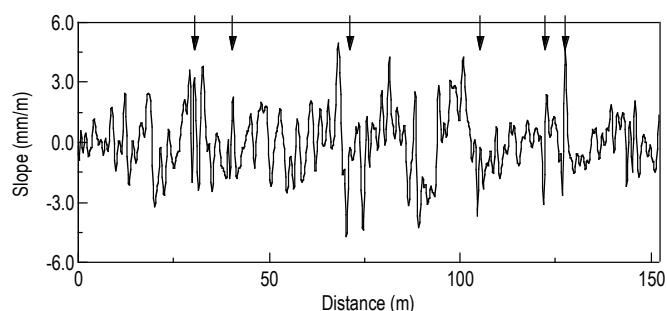

(a) l=29.7 m

(b) l=39.6m

(c) l=70.2 m

(d) l=104.7 m
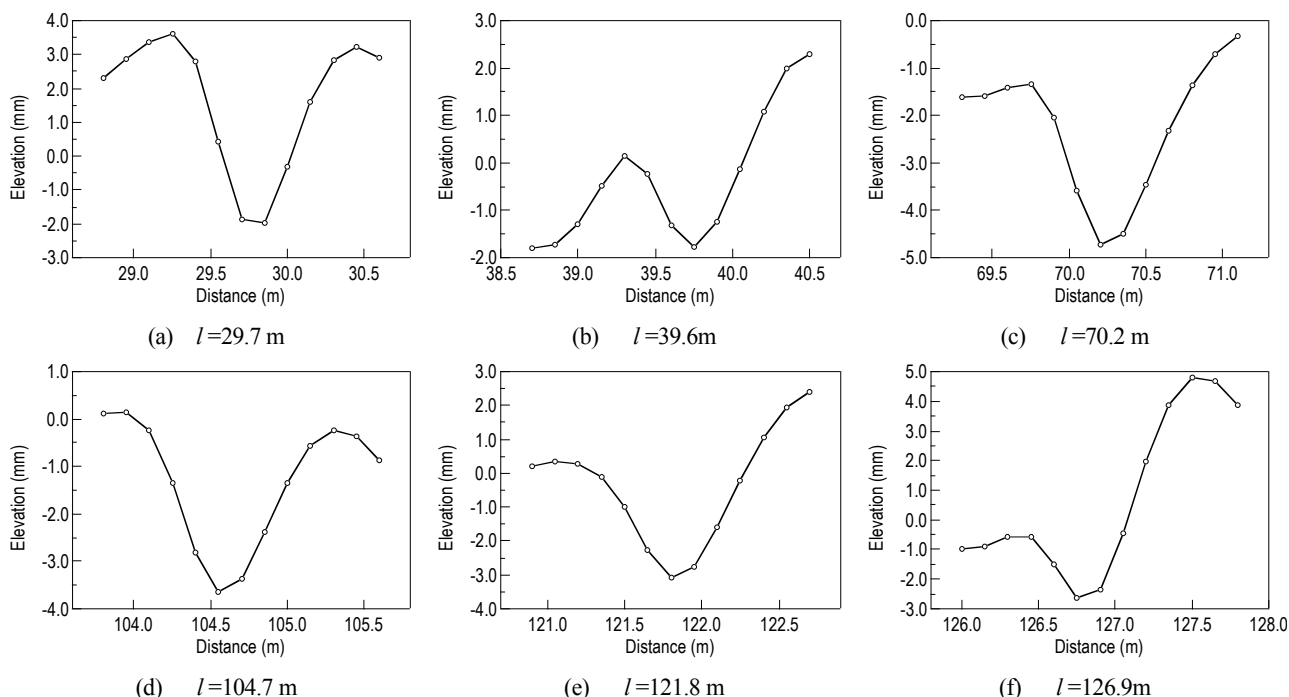
(e) l=121.8 m

(f) l=126.9m

Fig. 6. Training Signals.

Table 1. Initial Wavelet Filters.

k, m	$h_{k,l}^{old}$	$\tilde{h}_{k,l}^{old}$	$g_{m,l}^{old}$	$\tilde{g}_{m,l}^{old}$
0	0.7071	0.9944	-0.9944	-0.7071
1, -1	0.3536	0.4198	0.4198	0.3536
2, -2	-	-0.1768	0.1768	-
3, -3	-	-0.0663	-0.0663	-
4, -4	-	0.0331	-0.0331	-

and sharp spikes with similar profile shapes that are depicted in Fig. 6.

A set of Initial Wavelet Filters

A wide selection of basic function forms of wavelet transformations is available for different applications based on the characteristics of the signal concerned. In the present study, the biorthogonal reconstruction and decomposition filters with 2 and 4 vanishing moments were selected as a set of initial wavelet filters. This filter set consists of comparatively short digital filters, and is associated with the basic function that has a sharp peak. Although lifting wavelet filters can be constructed from arbitrary filter sets, the features of the initial wavelet filters are advantageous to deal with pavement cracks. Table 1 describes the set of initial wavelet filters.

Construction of Wavelet Filters

Lifting wavelet filters are adaptive biorthogonal wavelet filters containing controllable free parameters. In the present study, We learnt free parameters that control the initial filters to be suitable for the features of cracks using the training signals shown in Fig. 6. As the $c_l^{1,v}$ ($v = 1, 2, 3, 4, 5, 6$) denote the training signals, the number of free parameters $\tilde{S}_{k,m}$ can be determined by using Eq. (16). The matrix form in the equation is summarized as follows:

$$\begin{bmatrix} a_{m-3}^1 & a_{m-2}^1 & a_{m-1}^1 & a_m^1 & a_{m+1}^1 & a_{m+2}^1 & a_{m+3}^1 \\ a_{m-3}^2 & a_{m-2}^2 & a_{m-1}^2 & a_m^2 & a_{m+1}^2 & a_{m+2}^2 & a_{m+3}^2 \\ a_{m-3}^3 & a_{m-2}^3 & a_{m-1}^3 & a_m^3 & a_{m+1}^3 & a_{m+2}^3 & a_{m+3}^3 \\ a_{m-3}^4 & a_{m-2}^4 & a_{m-1}^4 & a_m^4 & a_{m+1}^4 & a_{m+2}^4 & a_{m+3}^4 \\ a_{m-3}^5 & a_{m-2}^5 & a_{m-1}^5 & a_m^5 & a_{m+1}^5 & a_{m+2}^5 & a_{m+3}^5 \\ a_{m-3}^6 & a_{m-2}^6 & a_{m-1}^6 & a_m^6 & a_{m+1}^6 & a_{m+2}^6 & a_{m+3}^6 \\ 1 & 1 & 1 & 1 & 1 & 1 & 1 \end{bmatrix} \begin{bmatrix} \tilde{s}_{m-3,m} \\ \tilde{s}_{m-2,m} \\ \tilde{s}_{m-1,m} \\ \tilde{s}_{m,m} \\ \tilde{s}_{m+1,m} \\ \tilde{s}_{m+2,m} \\ \tilde{s}_{m+3,m} \end{bmatrix} = \begin{bmatrix} r_m^1 \\ r_m^2 \\ r_m^3 \\ r_m^4 \\ r_m^5 \\ r_m^6 \\ 0 \end{bmatrix} \quad (18)$$

Table 2 indicates the leant free parameters $\tilde{S}_{k,m}$. Using these parameters, a set of adaptive filters $\{h_{k,l}, \tilde{h}_{k,l}, g_{m,l}, \tilde{g}_{m,l}\}$ has been created by using Eq. (6) as shown in Table 3.

Detection Result

Fig. 7 shows the result of automatic detection of the severe cracks. Where arrows mark the cracks. As shown in the figure, the adaptive filters clearly emphasize the locations that the feature is similar to the learnt cracks. The figure also indicates the same level of I_m

Table 2. Free Parameters.

K	$\tilde{s}_{k,m}$
m -3	-0.1111
m -2	0.1314
m -1	-0.0023
M	0.0391
m +1	-0.1426
m +2	0.1092
m+3	-0.0237

Table 3. Adaptive Lifting Wavelet Filters.

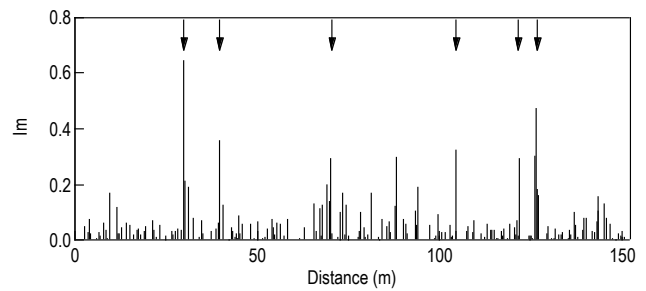| k, m	$h_{k,l}^{old}$	$\tilde{h}_{k,l}^{old}$	$g_{m,l}^{old}$	$\tilde{g}_{m,l}^{old}$
-4	-0.0505	0.0331	-0.0331	0.0505
-3	0.1689	-0.0663	-0.0663	0.1689
-2	-0.0150	-0.1768	0.1768	0.0150
-1	0.2143	0.4198	0.4198	0.2143
0	0.7524	0.9944	-0.9944	-0.7524
1	0.4012	0.4198	0.4198	0.4012
2	-0.0172	-0.1768	0.1768	0.0172
3	-0.0078	-0.0663	-0.0663	-0.0078
4	0.0016	0.0331	-0.0331	-0.0016

Fig. 7. Automatic Detection Result for Causative Cracks in Roughness.

value as the severe cracks at the distance of 88.2m because the shape of the profile is similar to the training signals. On the other hand, the adaptive filters do not respond locations where the cracks are not related to the pavement roughness cannot be detected. The locations that can be detected should be treated in respect to the pavement function as well as structure and materials. According to this result, we conclude that the lifting scheme is an effective method for detecting the cracks that have specific features in the roughness profile. This study contributes to automatic distress detection using response type profiling systems. Although this paper demonstrated the case of pavement cracks, adaptive wavelet filters that have different specifications can be developed by learning free parameters from various types of pavement distress such as pothole and patching as well as cracks.

Conclusions

This study illustrated an automatic detection method of localized surface roughness by developing lifting wavelet filters for the surface monitoring by use of QC-based response type systems. Lifting wavelet filters enable us to construct adaptive filters

containing controllable free parameters. In this paper, we designed a set of lifting wavelet filters for detecting causative localized distress such as transverse cracks in the QC filtered roughness profile. The free parameters were leant from six cracks in the profile stored in the LTPP database, and then the set of adaptive filters was developed for detecting the cracks that needs to be evaluated from functional point of view. This paper also provided an application case study to demonstrate the availability of the adaptive wavelet filters for the crack detection. According to the results, the adaptive filter clearly emphasized the locations of severe cracks that have the profile features similar to the learnt cracks. This performance of the lifting wavelet filters contributes to automatic distress detection using response type profiling systems. Although this paper demonstrated the case of pavement cracks, adaptive wavelet filters that have different specifications can be developed by learning free parameters from various types of pavement distress such as pothole and patching as well as cracks.

Acknowledgment

References

1. Tomiyama, K., Kawamura, A., Nakajima, S., Ishida, T., and Jomoto, M. (2001). A Mobile Data Collection System Using Accelerometers for Pavement Maintenance and Rehabilitation, *Proceedings of 8th International Conference on Managing Pavement Assets*, Santiago, Chile, Paper No. 142 (CD-ROM).

2. Fugal, D.L. (2009). *Conceptual Wavelets in Digital Signal Processing*, Space and Signals Technical Publishing, San Diego, CA, USA.

3. Daubechies, I. (1992). *Ten Lectures on Wavelets*, CBMS-NSF Conference Series in Applied Mathematics, Society for Industrial and Applied Mathematics, Philadelphia, PA, USA.

4. Wei, L., and Fwa, T.F. (2004). Characterizing Road Roughness By Wavelet Transform. *Transportation Research Record*, No. 1869, pp. 152-158.

5. Shokouhi, P., Gucunski, N., Maher, A., and Zaghloul, S.M. (2005). Wavelet-Based Multiresolution Analysis of Pavement Profiles as a Diagnostic Tool, *Transportation Research Record*, No. 1940, pp. 79-88.

6. Sweldens, W. (1997). The Lifting Scheme: A Construction of Second Generation Wavelets, *SIAM Journal on Mathematical Analysis*, 29(2), pp. 511-546.

7. Jansen, M., and Oonincx, P. (2004). *Second Generation Wavelets and Application*, Springer, London, UK.

8. Takano, T., Minamoto, H., Arimura, K., Niijima, T., Iyemori, T., and Araki, T. (1999). Automatic Detection of Geomagnetic Sudden Commencement using Lifting Wavelet Filters. *Proceedings of the Second International Conference on Discovery Science*, Tokyo, Japan, pp. 242-251.

9. Sayers, M.W. and Karamihas, S.M. (1998). The Little Book of Profiling, - Basic Information about Measuring and Inter-preting Road Profiles, The University of Michigan, Ann Arbor, Michigan, USA.

10. Von Quintus, H.L., Simpson, A.L., and Eltahan, A.A. (2006). Rehabilitation of Asphalt Concrete Pavements: Initial Evaluation of The SPS-5 Experiment—Final Report, Publication *FHWA-RD-01-168*. FHWA, U.S. Department of Transportation, Washington DC, USA.

11. LTPP Products Online (2012). *http://www.ltpp-products.com/*, Accessed July 2012.